Journal of the Optical Society of Korea, Vol. 1, No. 1, March 1997, pp. 26~35

Rigorous coupled-wave analysis of antireflective surface-relief gratings

Chang-Wook Han and Doo Jin Cho
Department of Physics, Ajou University, SuWon 442-749, Korea

Bum Ku Rhee
Department of Physics, Sogang University, Seoul 121-742, Korea

(Received; January 29, 1997)

Rigorous coupled-wave analysis(RCWA) with a simplified eigenvalue problem is used to investigate the antireflective property of one-dimensional surface-relief gratings such as binary gratings, triangular gratings and gratings with triangle-like surface profiles. The convergence of RCWA is investigated by varying the number of layers and the number of space-harmonics used in the computation. For unpolarized light normally incident on a medium of refractive index 1.64 from vacuum, a triangle-like grating shows the reflectivity of 1.6×10^{-4} in contrast to a minimum reflectivity of 3.8×10^{-3} for a binary grating. We also study the dependence of reflectivity on the wavelength, and on the angle of incidence for a groove shape and depth which result in minimum reflectivity.

I. INTRODUCTION

Diffraction gratings have received great attention due to their usefulness in many disciplines, such as optical information processing, optical computing, acousto-optics, integrated optics, holography, spectroscopy, etc[1-3]. Subwavelength structured(SWS) surfaces that contain diffraction gratings with a period significantly smaller than the wavelength of light do not show a diffraction effect. Only the zeroth transmitted and reflected orders propagate, i.e., all diffraction orders other than the zeroth order are evanescent: they are also called zeroth-order gratings. Therefore SWS surfaces behave like thin films whose refractive-index profile depends on their surface structure. With one-dimensional SWS grating, one can synthesize an artificial uniaxial thin film with the optic axis parallel to the grating vector, and a biaxial film can be obtained with a two-dimensional SWS grating. Thus, SWS gratings have been used as antireflection surfaces, polarization elements, narrow-band filters, wave plates, etc[4-6]. With maturing submicron- or nano-lithographic technology available to fabrication, these surfaces may significantly influence those aspects of thin-film optics technology that currently suffers from a lack of available materials.

Antireflective SWS gratings have been studied by numerous researchers[7-17]. Gaylord, *et al.*[9] considered the zero-reflectivity binary gratings, reporting a reflectivity less than 5×10^{-7}. Ono *et al.*[10] reported a reflectivity $<10^{-6}$ for a surface-relief grating with nearly triangular shape, assuming that it had circle-arc effective-index distribution according to their model, which was similar to the single-homogeneous-layer model[11,12]. Raguin and Morris[13] considered both one- dimensional and two-dimensional antireflection structured surfaces on GaAs substrates for the infrared spectral region. More recently, Grann *et al.*[15,16] showed that two-dimensional subwavelength binary gratings could suppress reflections over a broad range of wavelengths.

Among theories which can predict the characteristics of diffraction gratings accurately, the rigorous coupled-wave analysis(RCWA) has been most popular owing to its advantages[18-21]. In the RCWA for surface-relief gratings, the groove is divided into a number of layers, the electromagnetic field in each layer is expanded in terms of spatial harmonics, and Maxwell's equations are applied. While a considerable amount of time is usually taken to find results numerically with RCWA, it was shown that a reduction in the dimensions of the related matrix is always possible so that computing time and memory requirements for a computer can be greatly reduced[22].

In this research, we use the RCWA with a simplified eigenvalue problem to investigate the antireflective property of one-dimensional surface-relief gratings as a function of various parameters of the grating. In Section 2 the RCWA with a simplified eigenvalue problem for three-dimensional diffraction of arbitrarily polarized light from arbitrary two-dimensional surface-relief dielectric gratings is briefly presented. In Section 3 we study the convergence of RCWA, varying the number of layers and the number of space-harmonics used in the computation. Also, conditions for a minimum reflectivity are investigated for the various gratings such as binary gratings, triangular gratings and gratings with triangle-like surface profiles. In the case of a binary grating the filling factor and the groove depth are varied, and the groove shape and depth are

varied with a filling factor of 100% for the rest. We also investigate the dependence of reflectivity on the wavelength and the angle of incidence for a groove shape and depth which result in a minimum reflectivity.

II. RIGOROUS COUPLED-WAVE ANALYSIS WITH SIMPLIFIED EIGEN-VALUE PROBLEM

The general three-dimensional diffraction from a two-dimensional surface-relief grating with an arbitrary period is schematically shown in Fig. 1. An arbitrary polarized electromagnetic wave is obliquely incident at an angle (α, δ) on the grating which is in the xy-plane and whose groove depth is d. The grating has arbitrary periodicity directions represented by grating vectors vec $\vec{K}_1$ and vec $\vec{K}_2$. The grating consists of three regions: incidence region(I) is $z < 0$, modulated region(II) is $0 \le z \le d$, and transmission region(III) is $z > d$. The complex relative permittivity of regions I and III are denoted by ε_1 and ε_3, and that of region II is a function of x,y and z. When this region is divided into N layers, the complex relative permittivity of the ith layer $\varepsilon_{2,i}(x,y) = \varepsilon_2(x,y,z_i)$, where $z_i (i = 1,2,...,N)$ denotes the z-coordinate of the layer, can be expressed as a complex Fourier series

$$\varepsilon_{2,i}(x,y) = \sum_p \sum_q \tilde{\varepsilon}_{i,pq} \exp[j(\vec{p}\vec{K}_1 + \vec{q}\vec{K}_2)\cdot\vec{r}], \tag{1}$$

where p and q are integers, $\vec{r} = x\hat{x} + y\hat{y}$ and $j = \sqrt{-1}$. When the region II is divided into N layers of equal thickness, $z_i = id/N$. Throughout this work, the time dependence of electromagnetic field is assumed to be $e^{j\omega t}$.

1. Rigorous Coupled-wave analysis

In the RCWA, Maxwell's equations are solved in each region of space and boundary conditions for the tangential components of electric and magnetic fields are applied at each plane $z = z_i (i = 0,1,..,N)$. In regions I and III the electric field vectors can be expressed in terms of plane waves, i.e.,

$$\vec{E}_1 = \vec{E}_{inc} + \sum_m \sum_n \vec{R}_{mn} \exp(-j\vec{k}_{1,mn}\cdot\vec{r}), \tag{2a}$$

$$\vec{E}_3 = \sum_m \sum_n \vec{T}_{mn} \exp[-j\vec{k}_{3,}mn\cdot(\vec{r} - d\hat{z})], \tag{2b}$$

respectively, where $\vec{R}_{mn}$ and $\vec{T}_{mn}$ are normalized electric field vectors of the m, nth reflected and transmitted waves, respectively. $\vec{E}_{inc}$ is the electric field for the incident plane wave which can be expressed as

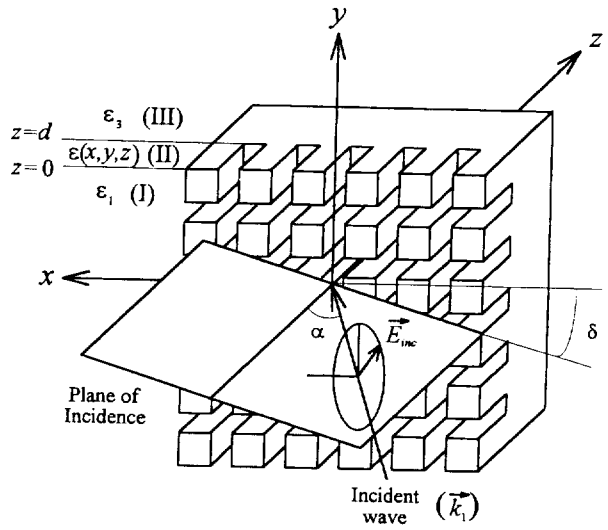

Fig 1. General three-dimensional diffraction of arbitrarily polarized light from an arbitrary two-dimensional surface-relief grating.

$$\vec{E}_{inc} = \hat{u}\exp(-j\vec{k}_1\cdot\vec{r}), \tag{3}$$

where $\vec{k}_1$ is the incident wave vector and $\hat{u}$ is the polarization unit vector. In Eqs.(2a) and (2b), phase matching and the Floquet theorem require t

$$\vec{k}_{l,mn} = k_{x,mn}\hat{x} + k_{y,mn}\hat{y} + k_{z,l,mn}\hat{z}, \quad (l = 1,3) \tag{4}$$

where

$$k_{x,mn} = k_1 \sin\alpha\cos\delta - (mK_{x,1} + nK_{x,2}), \tag{5a}$$

$$k_{y,mn} = k_1 \sin\alpha\sin\delta - (mK_{y,1} + nK_{y,2}), \tag{5b}$$

$$k_{z,l,mn} = \sqrt{k_l^2 - k_{x,mn}^2 - k_{y,mn}^2} \tag{5c}$$

with $k_l = 2\frac{\pi}{\lambda}\sqrt{\varepsilon_l}$. Here, λ is the free-space wavelength.

In the ith layer of region II, the electric and magnetic fields are expanded in terms of space-harmonic fields as

$$\vec{E}_{2,i} = \sum_m \sum_n [S_{x,i,mn}(z)\hat{x} + S_{y,i,mn}(z)\hat{y} + S_{z,i,mn}(z)\hat{z}] \exp(-j\vec{k}_{2,i,mn}\cdot\vec{r}), \tag{6}$$

$$\vec{H}_{2,i} = \sqrt{\frac{\varepsilon_0}{\mu_0}} \sum_m \sum_n [U_{x,i,mn}(z)\hat{x} + U_{y,i,mn}(z)\hat{y} + U_{z,i,mn}(z)\hat{z}] \times \exp(-j\vec{k}_{2,i,mn}\cdot\vec{r}), \tag{7}$$

where ε_0 is the permittivity of free space, 0 is the permeability of free space, which is the assumed permeability in all regions, $\vec{S}_{i,mn}(z)$ and $\vec{U}_{i,mn}(z)$ are the normalized amplitudes of the m, nth space-harmonic electric and magnetic fields, and $\vec{k}_{2,i,mn}$ is given by

$$\vec{k}_{2,i,mn} = k_{x,mn}\hat{x} + k_{y,mn}\hat{y} + k_{z,i}\hat{z}, \tag{8}$$

due to the Floquet theorem and the phase matching condition. Here,

$$k_{z,i} = [k^2\overline{\varepsilon_{2,i}} - k_1^2 \sin^2\alpha]^{1/2}, \tag{9}$$

where $\overline{\varepsilon_{2,i}}$ denotes the average relative permittivity of the ith layer and $k = \omega/c = 2\pi/\lambda$ is the wave number in vacuum. If we denote the maximum value of m and n by M, then $L = (2M+1)^2$ is the number of space-harmonic fields used in the computation.

Substituting $\varepsilon_{2,i}$, its inverse, $\vec{E}_{2,i}$ and $\vec{H}_{2,i}$ given by Eq.(1), Eq.(6) and Eq.(7) into Maxwell's equations, i.e.,

$$\nabla \times \vec{E}_{2,i} = -j\omega\mu_0 \vec{H}_{2,i}, \tag{10}$$

$$\nabla \times \vec{H}_{2,i} = j\omega\varepsilon_0 \varepsilon_{2,i}(x,y)\vec{E}_{2,i}, \tag{11}$$

we obtain the first-order coupled-wave equations which can be written in the matrix form

$$\frac{d\mathbf{V}_i}{dz} = j\mathbf{A}_i\mathbf{V}_i, \tag{12}$$

wherermbold $\mathbf{V}_i$ and $\mathbf{A}_i$ is the vector with $4L$ components and the $4L \times 4L$ matrix which can be written as

$$\mathbf{V}_i = (\mathbf{S}_{x,i}\,\mathbf{S}_{y,i}\,\mathbf{U}_{x,i}\,\mathbf{U}_{y,i})^T, \tag{13}$$

$$\mathbf{A}_i = k_{z,i}\mathbf{I} + \begin{pmatrix} 0 & 0 & \mathbf{a}_i & \mathbf{b}_i \\ 0 & 0 & \mathbf{c}_i & \mathbf{d}_i \\ \mathbf{e} & \mathbf{f}_i & 0 & 0 \\ \mathbf{g}_i & -\mathbf{e} & 0 & 0 \end{pmatrix} \tag{14}$$

Here T, $\mathbf{I}$, $\mathbf{0}$, $\mathbf{S}_{x,i}$, $\mathbf{S}_{y,i}$, $\mathbf{U}_{x,i}$, $\mathbf{U}_{y,i}$ denotes the transpose, the unix matrix, the zero matrix, the matrices whose m, n-th components given by $S_{x,i,mn}(z)$, $S_{y,i,mn}(z)$, $U_{x,i,mn}(z)$, and $U_{y,i,mn}(z)$ respectively and $\mathbf{a}_i$, $\mathbf{b}_i$, $\mathbf{c}_i$, $\mathbf{d}_i$, $\mathbf{e}$, $\mathbf{f}_i$ and $\mathbf{g}_i$ are the sub-matrices (For details, refer to Ref).[22]

In general, Eq.(12) is solved by using the state-variable method. Denoting eigenvalues of $\mathbf{A}_i$ $\lambda_{i,r}$ and the corresponding eigenvectors ($\mathbf{w}_{1,i,r}$ $\mathbf{w}_{2,i,r}$ $\mathbf{w}_{3,i,r}$ $\mathbf{w}_{4,i,r}$)^T, we can express the final solution as the following forms, i. e.,

$$\mathbf{S}_{x,i}(z) = \sum_{r=1}^{4L} C_{i,r}\mathbf{w}_{1,i,r}\, exp(j\lambda_{i,r}z), \tag{15a}$$

$$\mathbf{S}_{y,i}(z) = \sum_{r=1}^{4L} C_{i,r}\mathbf{w}_{2,i,r}\, exp(j\lambda_{i,r}z), \tag{15b}$$

$$\mathbf{U}_{x,i}(z) = \sum_{r=1}^{4L} C_{i,r}\mathbf{w}_{3,i,r}\, exp(j\lambda_{i,r}z), \tag{15c}$$

$$\mathbf{U}_{x,i}(z) = \sum_{r=1}^{4L} C_{i,r}\mathbf{w}_{4,i,r}\, exp(j\lambda_{i,r}z), \tag{15d}$$

where $C_{i,r}$ represents the constants of integration.

There are (4N+6)L unknowns which account for $3L\vec{R}_{mn}$'s, $3L\vec{T}_{mn}$'s and $4NLC_{i,r}$'s. These can be determined by the same number of equations which are given by 4(N+1)L boundary conditions for the tangential components of $\vec{E}$ and $\vec{H}$ on $(N+1)$ planes at z_i $(i = 0,1,\cdots,N)$ and the Maxwell's equation $\nabla\cdot(\varepsilon\vec{E}) = 0$ in regions I and III. Gaussian elimination can be used for effective computation of unknowns. Therefore for arbitrary surface-relief gratings we can obtain rigorous results with a finite number of layers, and we determine the number of space-harmonics numerically.

For one-dimensional grating whose antireflective properties are studied in this work, equations discussed above can be used with the following simplification. First of all, the grating can be represented by a single grating vector $\vec{K}$ instead of two. Also only one index m corresponding to the mth reflected transmitted waves and space-harmonic fields, instead of two indices m and n, is necessary. Therefore Eqs.(4) and (5) are modified to

$$\vec{k}_{l,m} = k_{x,m}\hat{x} + k_y\hat{y} + k_{z,l,m}\hat{z}, \quad (l = 1,3) \tag{4'}$$

where

$$k_{x,m} = k_1 \sin\alpha\cos\delta - mK, \tag{5a'}$$

$$k_y = k_1 \sin\alpha \sin\delta, \tag{5b'}$$

$$k_{z,l,m} = \sqrt{k_l^2 - k_{x,m}^2 - k_y^2}, \tag{5c'}$$

and the grating vector $\vec{K}$ is assumed to be in the x-direction.

2. Simplified eigenvalue problem

In general, most of the computing time for calculationg electromagnetic fields for reflected and transmitted waves is used up for obtaining eigenvalues and eigenvectors of coefficient matricesrmbold $\mathbf{A}_i$ in Eq.(14). However, this eigenvalue problem can always be simplified due to the particular structure of the matrix.[22]

Let's consider a block matrix of the following from

$$\mathbf{A} = \begin{pmatrix} \beta\mathbf{I} & \mathbf{A}_{s1} \\ \mathbf{A}_{s2} & \beta\mathbf{I} \end{pmatrix} \tag{16}$$

where β is a constant which corresponds to $k_{z,i}$, $\mathbf{A}_{s1}$ $\mathbf{A}_{s2}$ are sub-matrices which can be written as,

$$\mathbf{A}_{s1} = \begin{pmatrix} a_i & b_i \\ c_i & d_i \end{pmatrix}, \tag{17a}$$

$$\mathbf{A}_{s2} = \begin{pmatrix} e & f_i \\ g_i & -e \end{pmatrix}. \tag{17b}$$

The eigenvalue equation forrmbold **A** can be expressed as

$$\mathbf{A}\begin{pmatrix} \mathbf{X}_1 \\ \mathbf{X}_2 \end{pmatrix} = \mathbf{A}\begin{pmatrix} \mathbf{X}_1 \\ \mathbf{X}_2 \end{pmatrix} \tag{18}$$

where Δ and $(\mathrm{X}_1^T\ \mathrm{X}_2^{T)^t}$ are the eigenvalue and the eigenvector, respectively. Eq.(18) can be rewritten as

$$\mathbf{A}_{s1}\mathbf{X}_2 = (\Delta - \beta)\mathbf{X}_1\ , \tag{19a}$$

$$\mathbf{A}_{s2}\mathbf{X}_1 = (\Delta - \beta)\mathbf{X}_2\ . \tag{19b}$$

By multiplyingrm $\mathbf{A}_{s1}$ to Eq.(19b) and substituting Eq. (19a), we obtain

$$\mathbf{A}_{s1}\mathbf{A}_{s2}\mathbf{X}_1 = (\Delta - \beta)^2\mathbf{X}_1\ , \tag{20}$$

which is the eigenvalue equation for the product matrix $\mathbf{A}_{s1}\mathbf{A}_{s2}$.

As can be seen above, the simplification of the eigenvalue problem is possible for the case when the diagonal block matrices $k_{z,i}\mathbf{I}$ of $\mathbf{A}_i$ are proportional to the unit matrix. In the case of volume diffraction gratings, this kind of simplification can not be obtained even in the simplest case.

The simplification of the eigenvalue problem discussed above is essential for reducing a computation time for obtaining diffraction characteristics of arbitrary surface-relief gratings. For example, in the case of **M** = *4* where 81 spatial harmonics are involved, the simplified eigenvalue problem for the 162×162 matrix $\mathbf{A}_{s1}\mathbf{A}_2$ requires 16 minutes for 486DX2-33 using cg from netlib,[23] in contrast to 2 hours and 36 minutes for the 324×324 matrix $\mathbf{A}_i$ which is about 10 times slower. When many layers are required to achieve accurate results, reduction in computing time will be much greater. This is very important considering the fact that the RCWA suffers from slow convergence in some situations.[4,24]

IV. ANTIREFLECTIVE PROPERTIES OF SWS GRATINGS

In general, diffraction characteristics of a grating including its reflectivity depend on the various parameters of grating such as surface shape, groove depth, filling factor and refractive index as well as the various conditions of incident light such as wavelength, angle of incidence and polarization. In particular, we consider binary gratings, triangular gratings and gratings with triangle-like surface profiles in order to find conditions for minimum reflectivity. The plane wave with a wavelength of 632.8 nm is normally incident on the surface- relief grating with refractive index of 1. 64(photoresist) and a period of 310 nm from vacuum. For polarization of the incident wave, we consider the TE, TM and random polarization(or unpolarized). The TE polarization refers to the situation where the electric vector of the incident light is orthogonal to the grating vector. The reflectivity for an unpolarized wave is obtained by averaging TE and TM reflectivity.

We first investigate the convergence of RCWA by varying the number of layers and the number of space-harmonics used in the computation. Then, we study the reflectivity of binary gratings varying the filling factor and the groove depth. With a filling factor of 100%, the groove shape and depth are varied for triangular gratings and gratings with triangle-like surface profiles. Surface shapes for triangle-like gratings are shown in Fig. 2(a) and (b), which will be explained in Section c. Finally, we also study the dependence of reflectivity on the wavelength and the angle of incidence for triangle-like gratings with a groove shape and depth which result in minimum reflectivity.

1. Convergence of RCWA

In order to determine the number of layers and the number of space-harmonics used in the computation that give a satisfactory performance, we have performed extensive computations for triangular and triangle-like gratings. The numbers of layers, N are 30, 50, 80, 100, 150, and 200, and M are 5, 10 and 15 for TE polarization and 10, 15, 20 and 30 for TM polarization. Note that for a one-dimensional grating, the number of space-harmonics, L is related to M by $L = 2M + 1$. We performed the computation for groove depths of 260 and 450 nm chosen arbitrarily. Since the behavior for the convergence shows a similar pattern, we only show the result for one representative case in the following.

Regarding convergence with respect to the number of space-harmonics, we considered the triangle-like grating of R1 = 2 (See Fig. 2 and Section c). The number of layers used are 30, 50, and 80. As can be seen in the table 1, for TE polarization, as the number of space-harmonics increases, the reflectivity decreases. When it varies from 5 to 10, the relative change for

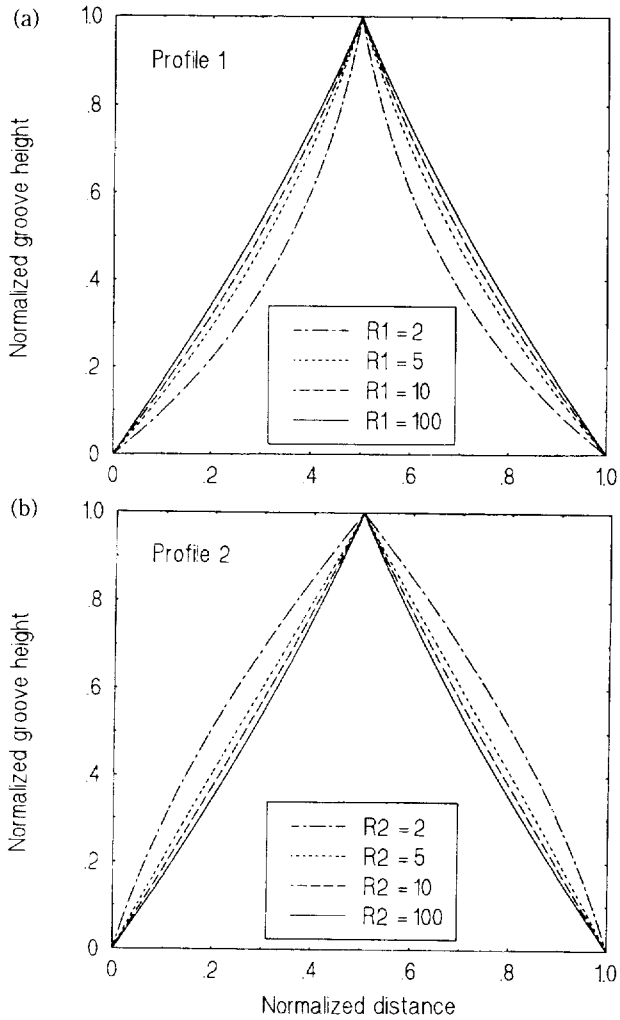

Fig. 2. Surface-profiles of triangle-like gratings. (a) R1; (b) R2. R 1-type is sharper than the profile with R = ∞.

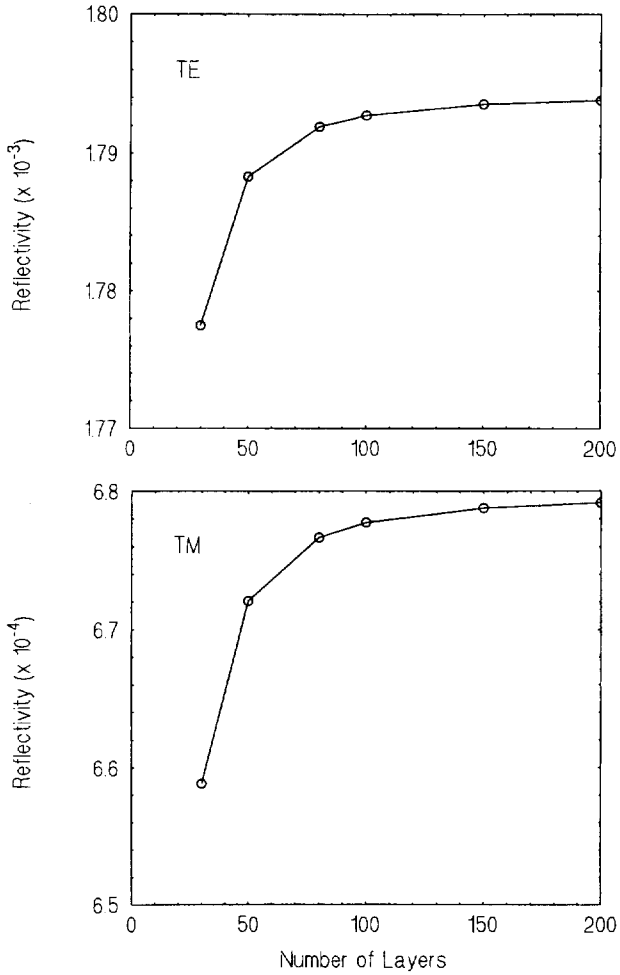

Fig. 3. Convergence for triangular grating with the groove depth 450 nm with respect to the number of layers: (a) TE polarization, number of space-harmonics 5; (b) TM polarization, number of space-harmonics 10.

the reflectivity is approximately 10^{-5}, and 10^{-6} for 10 and 15.

As pointed out by Li *et al.*[23], convergence with respect to the number of space-harmonics for TM polarization is much slower than that for TE polarization. As can be seen in the table 2, when the number of space-harmonics varies from 10 to 15, the relative change for the reflectivity is approximately 3~6.5%, 1.8~2.9% for 15 and 20, and 1.6~2.6% for 20 and 30. In contrast to the case of TE polarization, as the number of space-harmonics increases, the reflectivity for the groove depth of 260 nm increases, but that for 450 nm decreases. However, it is thought that this is only accidental. Actually the dependence of the reflectivity on the number of space-harmonics is not fixed: sometimes it increases as the number of space-harmonics increases, but sometimes it also decreases. Summarizing the study of convergence with respect to the number of space-harmonics, considering both accuracy and computing time, it is sufficient to take 5 for TE polarization, and 10 for TM case.

Regarding convergence with respect to the number of layers, we show the result for a triangular grating of groove depth 450 nm. In Fig. 3, the reflectivities for TE and TM polarizations are plotted against the number of layers. For TE polarization, the number of space-harmonics is 5, and 10 for TM case. Under the given conditions, we see that the reflectivities for both TE and TM polarizations increase as the number of layers increases. Unlike the convergence with respect to the number of space-harmonics, the behavior for different numbers of layers can be viewed as identical to the behavior with different surface-profiles. In other words, as the number of layers increases, we have gratings of different surface profiles. In any case, in order to represent the surface shape of triangular gratings adequately, considering the convergence and the computation time, we need about 100 layers. Since this is also true for triangle-like surface profiles, 100 layers

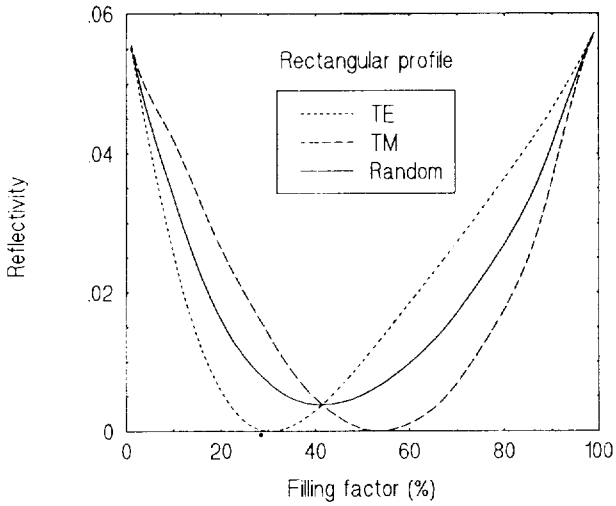

Fig. 4. For a binary grating, reflectivities for TE, TM, and unpolarized(random) light are shown as a function of the filling factor.

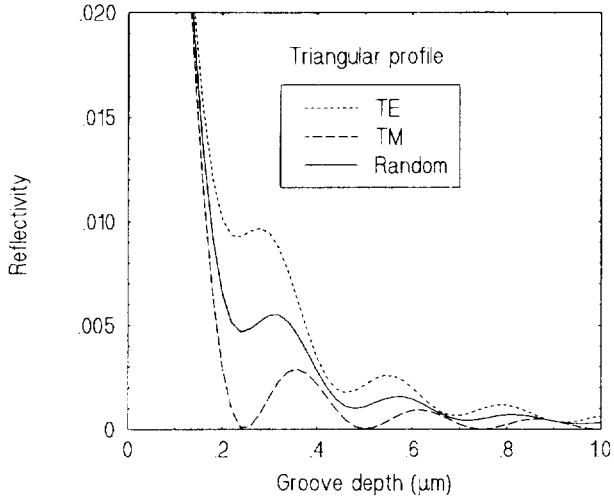

Fig. 5. For a triangular grating, reflectivities for TE, TM, and unpolarized(random) light are shown as a function of the groove depth.

are used in the rest of this research except for the case of binary gratings.

2. Binary Gratings and Triangular Gratings

Many researchers have studied diffraction characteristics of binary or rectangular gratings and triangular gratings. Here we study them in order to verify the performance of the RCWA computer program and to compare results with those of triangle-like gratings. In the case of binary gratings, the filling factor and the groove depth are varied in order to find conditions for a minimum reflectivity. For triangular gratings, the groove depth is varied with a filling factor of 100%.

In Fig. 4, minimum reflectivity for binary gratings is shown as a function of filling factor which varies from 1 to 100%. For TE polarized light, the number of space-harmonics is 5, and 10 for TM case. For a given value of the filling factor, minimum reflectivity is obtained by varying the groove depth from 20 nm to 1 m. The lowest minimum reflectivity for TE polarized light is found to be 7.0×10^{-6} at the filling factor of 31%, and that for TM light 6.1×10^{-6} at the filling factor of 53%. These are comparable to reflectivities for gratings of other surface-profiles. However, the lowest minimum reflectivity for unpolarized (or random) light obtained by averaging TE and TM minimum reflectivities is found to be 3.8×10^{-3} at the filling factor of 41%.

In Fig. 5, reflectivity for triangular gratings is plotted as a function of groove depth. The filling factor is 100% and the number of layers is 100 with other parameters remained unchanged. The reflectivity shows oscillations with minimum values getting smaller as the groove becomes deeper.

Table 1. Convergence for triangle-like grating of R1 = 2. TE polarization.

# of layers	groove depth (nm)	# space-harmonics	reflectivity
30	260	5	0.01450653
		10	0.01450550
		15	0.01450542
	450	5	0.00464992
		10	0.00464912
		15	0.00464904
50	260	5	0.01454122
		10	0.01454009
		15	0.01453999
	450	5	0.00466411
		10	0.00466353
		15	0.00466346
80	260	5	0.01456024
		10	0.01455906
		15	0.01455896
	450	5	0.00468492
		10	0.00468447
		15	0.00468441

3. Triangle-Like Gratings

Ono *et al.*[10] reported a very low reflectivity $<10^{-4}$% for a surface-relief grating with nearly triangular shape, assuming that it had circle-arc effective-index distribution according to the single-homogeneous-layer model[11,12]. The single-homogeneous-layer model assumes that the groove region of the binary grating can be treated as a single homogeneous layer of the same thickness. The effective refractive index of the layer depends on the polarization of incident light. For TE po-

Table 2. Convergence for triangle-like grating of R1 = 2. TM polarization.

# of layers	groove depth (nm)	# space-harmonics	reflectivity
30	260	10	0.001846
		15	0.001923
		20	0.001959
		30	0.001992
	450	10	0.000453
		15	0.000425
		20	0.000413
		30	0.000406
50	260	10	0.001737
		15	0.001810
		20	0.001848
		30	0.001885
	450	10	0.000557
		15	0.000520
		20	0.000505
		30	0.000492
80	260	10	0.001683
		15	0.001754
		20	0.001790
		30	0.001826
	450	10	0.000624
		15	0.000583
		20	0.000566
		30	0.000551

larization, it is given by

$$n_{\overline{TE}} = \sqrt{n_1^2 (1-F) + n_2^2 F} \ , \tag{24}$$

and

$$\overline{n_{TM}} = \frac{n_1 n_2}{\sqrt{n_2^2 (1-F) + n_1^2 F}} \tag{25}$$

for TM polarization, where n_1 and n_2 are refractive indices of incident and transmitting media, respectively and F denotes the filling factor of the layer.

In Fig. 2, the groove profiles for the assumed circle-arc effective-index distribution are shown, where the effective refractive index has a depth profile with a circle-arc distribution. In Fig. 2(a), Eq.(24) is used to calculate the groove profile with the radius denoted by R1, and in Fig. 2(b), Eq.(25) is used with the radius denoted by R2. Profiles with smallest radius are at the extreme, i.e., R1=2 has the sharpest peak and R2 = 2 the widest. For a large value of the radius, e.g. R1 = R2 = 100, the two profiles become almost indistinguishable. The profile of R1-type is sharper than the profile with R = ∞. Note that the profile with R2 = 5 is very close to that of a triangular grating. As shown in Fig. 2, we only consider symmetric groove profiles with the filling factor 100%.

Table 3. Minimum reflectivities for triangle-like surface-relief gratings. The asterisk denotes the lowest reflectivity for TE and TM polarizations, respectively.

Surface-profile	Polarization	Reflectivity	Groove depth (nm)
R1 = 2	TE	2.2×10^{-5}	980
	TM	4.5×10^{-4}	1000
R2 = 2	TE	1.0×10^{-3}	900
	TM	4.0×10^{-5}	980
R1 = 5	TE	$*1.9\times10^{-5}$	940
	TM	1.6×10^{-4}	1000
R2 = 5	TE	3.3×10^{-4}	920
	TM	$*6.0\times10^{-6}$	740
R1 = 10	TE	5.5×10^{-5}	940
	TM	9.6×10^{-5}	1000
R2 = 10	TE	2.0×10^{-4}	920
	TM	2.5×10^{-5}	1000
R1 = 100	TE	1.1×10^{-4}	920
	TM	8.5×10^{-5}	1000
R2 = 100	TE	1.2×10^{-4}	920
	TM	4.8×10^{-5}	1000
Triangular	TE	3.3×10^{-4}	920
	TM	8.7×10^{-6}	1000

For triangle-like gratings with surface-profiles shown in Fig. 2(a) and (b), reflectivity is calculated using the RCWA, varying the groove depth up to 1 m in a step of 20 nm. In the Table 3, minimum reflectivity for each profile is shown for both TE and TM polarizations. The lowest reflectivity for TE polarization is 1.9×10^{-5} for R1 = 5 profile with the groove depth 940 nm, and that for TM polarization 6.0×10^{-6} for R2 = 5 profile with the groove depth 740 nm. In most cases, minimum reflectivity is obtained at deep groove close to 1 m. The lowest reflectivity in this work is higher than that of the value < 10^{-4} % reported by Ono *et al.* This result can be understood in the following way. When the grating has a period comparable to the wavelength of light, the single-homogeneous-layer model does not give good predictions. Notice that in this work the grating period 310 nm is about twice the wavelength(632.8 nm).

In Fig. 6(a)-(h), reflectivities for triangle-like gratings with different values of R1 and R2 are plotted against the groove depth. We found that, similar to triangular grating, reflectivity oscillates with minimum values getting smaller as the groove becomes deeper. From Fig. 6, we observe the following general features. As the profile becomes sharper, i.e., the smaller R1 and the larger R2, the TE reflectivity becomes lower, and in general, the difference between TE and TM reflectivities becomes smaller. R1 = 2 profile which has the sharpest peak shows the lowest reflectivity in the case of TE polarization. The TM reflectivity does not show as much variation as the profile

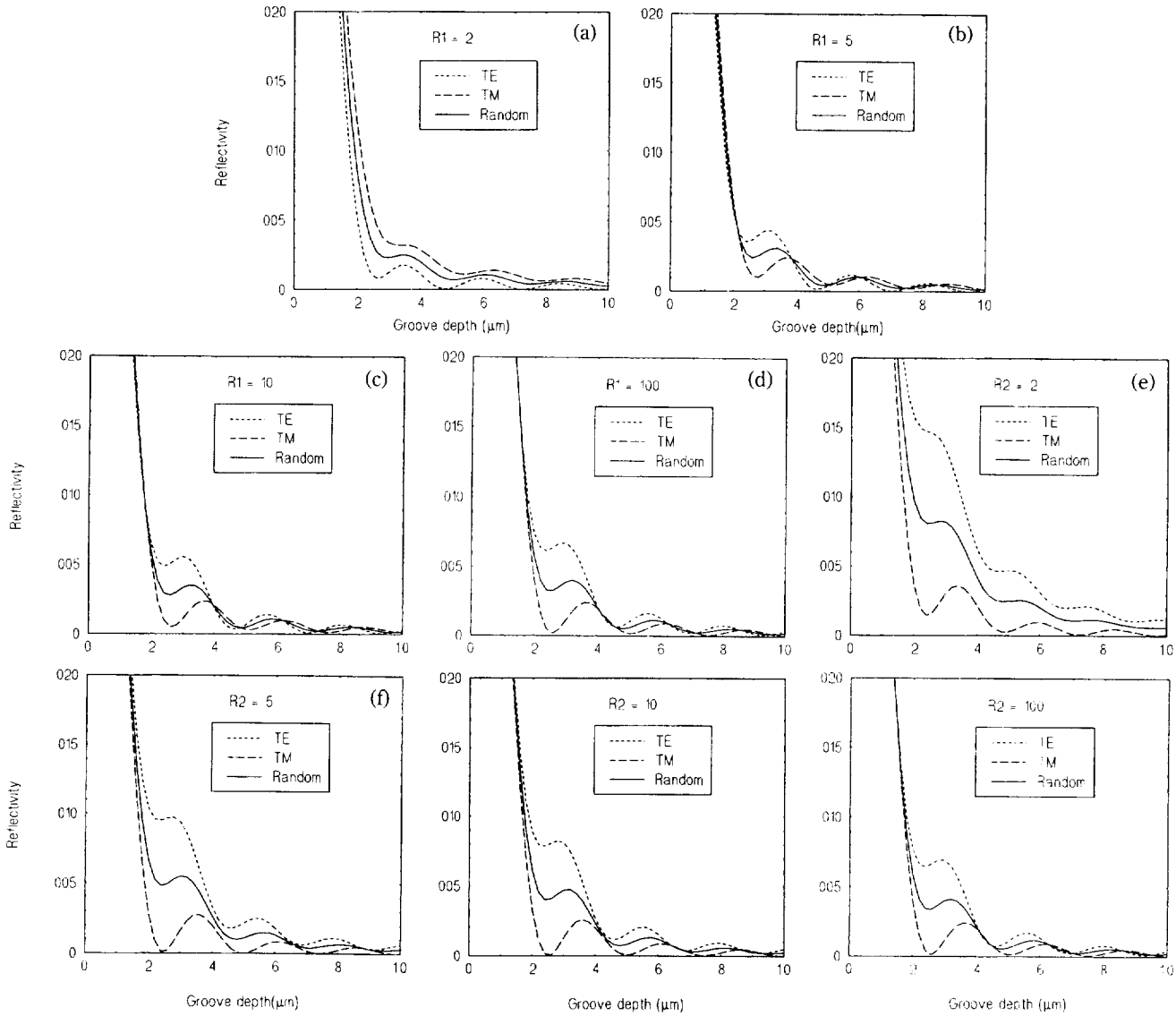

Fig. 6. For triangle-like gratings with various groove shapes (R=2, 5, 10, 100), reflectivities for TE, TM, and unpolarized light are plotted as a function of the groove depth. (a-d) R1; (e-h) R2.

changes. For all profiles, the deeper the groove, the smaller the difference between TE and TM reflectivities. We also found that the profile R2 = 2, which is more convex than the triangle, does not exhibit low reflectivity compared with other profiles. Since the profile with R2 = 5 is very close to a triangular grating, reflectivity shows an almost identical behavior. In general, R1-type gratings have a lower reflectivity than R2-type. Since the surface-profile for R1-type approaches that for R2-type as R becomes large, the reflectivities for R1 = 100 and R2 = 100 show similar behavior.

Since it is of practical interest to know the antireflective behavior for unpolarized(or random) light, we group curves for unpolarized reflectivity together in Fig. 7(a) and (b). As the profile becomes sharper, i.e., the smaller R1 and the larger R2, the unpolarized reflectivity becomes lower except for the case of R1 = 2. The lowest reflectivity 1.6×10^{-4} for unpolarized light is obtained for the profile with R1 = 5 at the groove depth 940 nm. As can be seen from Fig. 7, the profile with R1 = 5 has lower reflectivity than the triangular grating. Comparing the lowest reflectivity with that of 3.8×10^{-3} for a binary grating, we observe that triangle-like gratings show a superior antireflective performance for unpolarized light, although a binary grating performs better for TE polarization.

4. Dependence of Reflectivities on Wavelength and Angle of Incidenece for Triangle-Like Gratings

We also investigate the dependence of reflectivity on the wavelength and the angle of incidence for the triangle-like gratings with a groove shape and depth resulting in minimum reflectivity. As noted in Table 3, for

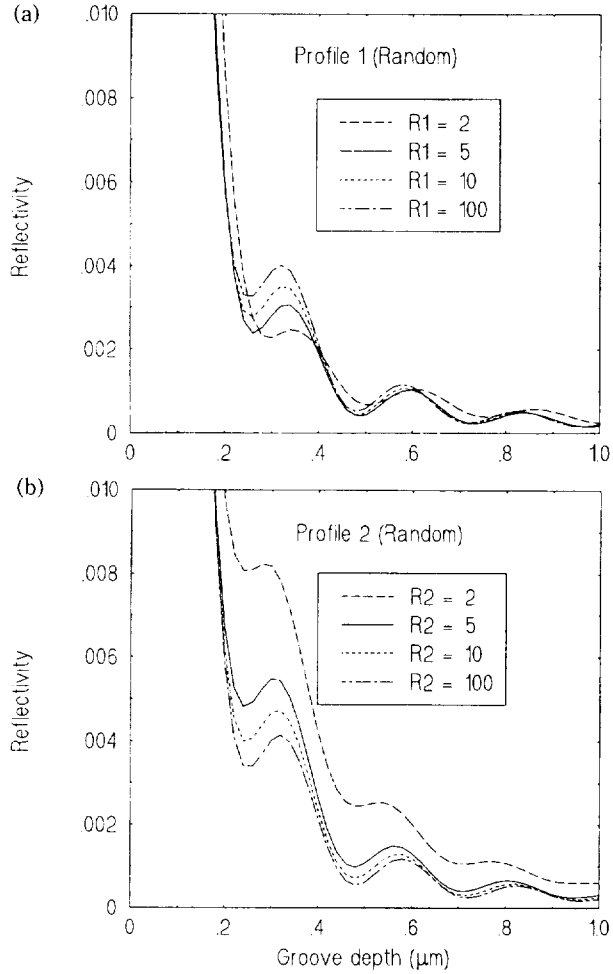

Fig. 7. For triangle-like gratings with various groove shapes and unpolarized light, reflectivities are plotted as a function of the groove depth. (a) R1; (b) R2.

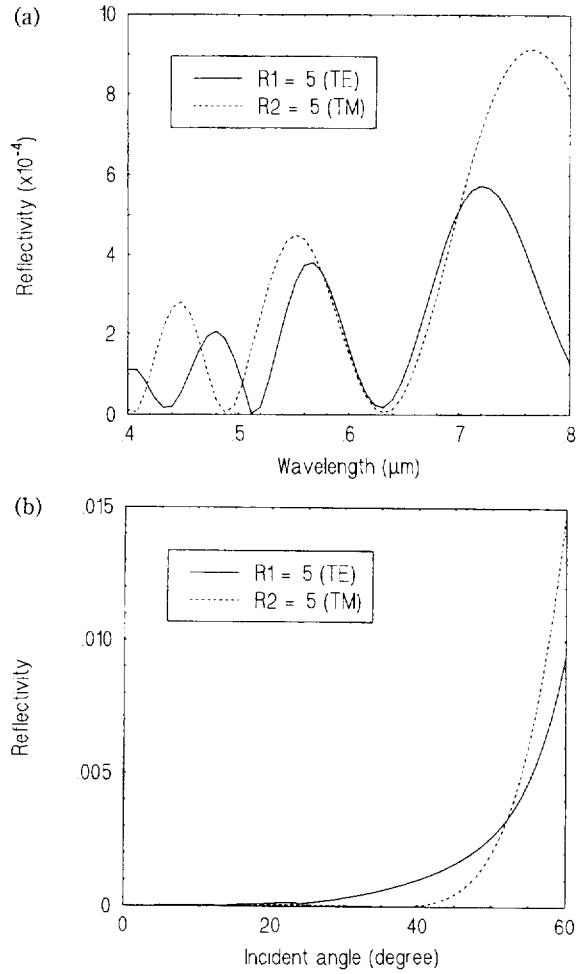

Fig. 8. For triangle-like gratings with the groove shape and depth resulting in minimum reflectivity, reflectivities are plotted as functions of (a) wavelength; (b) angle of incidence. Solid curves correspond to TE polarization, and broken curves to TM polarization.

TE polarization, the profile R1 = 5 with a groove depth 940 nm has a minimum reflectivity, and for TM polarization this occurs for the profile R2 = 5 with a groove depth 740 nm. In Fig. 8(a), reflectivity is plotted against wavelength. For TE polarization, the relative change in reflectivity is less than 0.06%, and for TM polarization, less than 0.1%, in the wavelength range from 400 nm to 800 nm. In Fig. 8(b), reflectivity is shown as a function of the angle of incidence, and the relative change in reflectivity with respect to the angle of incidence is less than 0.1% up to 40° for TE polarization, and less than 0.02% up to 43° for TM polarization. It can be concluded that antireflective properties of triangle-like gratings are insensitive to changes in wavelength and in the angle of incidence.

V. SUMMARY

In this work, the RCWA with a simplified eigenvalue problem is used to investigate the antireflective property of one-dimensional binary gratings, triangular gratings and gratings with triangle-like surface profiles. We first investigate the convergence of RCWA by varying the number of layers and the number of space-harmonics used in the computation. For TE polarization, it is sufficient to use 5 for the number of space-harmonics, and for TM, 10. For the number of layers in triangular gratings and in triangle-like gratings, 100 layers are sufficient to represent surface profiles.

Antireflective properties for gratings of a period of 310 nm are studied for light of wavelength 632.8 nm incident normally upon a medium of refractive index 1.64 from vacuum. For TE polarization, the lowest reflectivity among all gratings is found to be 7.0×10^{-6} for binary grating with a filling factor of 31%. On the other hand, for TM polarization, the minimum reflectivity is 6.0×10^{-6} for triangle-like grating with R2 = 5 and groove depth of 740 nm. For unpolarized light, a triangle-like grating shows the reflectivity of 1.6×10^{-4}

in contrast to a minimum reflectivity of 3.8×10^{-3} for a binary grating.

We also investigate the dependence of reflectivity on the wavelength and the angle of incidence for triangle-like gratings with a groove shape and depth which result in minimum reflectivity. For TE polarization, R1 = 5 with a groove depth 940 nm, and for TM polarization R2 = 5 with a groove depth 740 nm. For TE polarization, the relative change of the reflectivity is less than 0.06%, and for TM polarization, it is less than 0.1% in the wavelength range from 400 nm to 800 nm. In the case of the relative change in the reflectivity with respect to the angle of incidence, it is less than 0.1% up to 40° for TE polarization, and less than 0.02% up to 43° for TM polarization.

VI. ACKNOWLEDGMENTS

The present studies were supported by the Basic Science Reserch Institute Program, Ministry of Education, 1996, Project No. BSRI 96-2415.

REFERENCES

[1] R. Petit, Ed., *Electromagnetic Theory of Gratings*, Topics in Current Physics, Vol.**22** (Springer-Verlag, Berlin, 1980).

[2] T. K. Gaylord and M. G. Moharam, "Analysis and Applications of Optical Diffraction by Gratings," Proc. IEEE **73**, 894-937 (1985).

[3] D. Maystre, *Selected papers on diffraction gratings*, SPIE Milestone Series Vol. MS83 (SPIE, Bellingham, 1993).

[4] E. N. Glytsis, T. K. Gaylord, and D. L. Brundrett, "Rigorous coupled-wave analysis and applications of grating diffraction," in *Diffractive and Miniaturized Optics*, Critical Reviews of Optical Science and Technology Vol. CR 49, S. H. Lee, ed. (SPIE, Bellingham, 1993) pp.3-31.

[5] D. H. Raguin, S. Norton and G. M. Morris, "Subwavelength structured surfaces and their applications," in *Diffractive and Miniaturized* Optics, Critical Reviews of Optical Science and Technology Vol. CR49, S. H. Lee, ed. (SPIE, Bellingham, 1993) pp.234-261.

[6] P. Kipfer, M. Collischon, H. Haidner, and J. Schwider, "Subwavelength structures and their use in diffractive optics," Opt. Eng. **35**, 726-731 (1996).

[7] W. H. Southwell, "Pyramid-array surface-relief structures producing antireflection index matching on optical surfaces," J. Opt. Soc. Am. A8, 549-553 (1991).

[8] M. E. Motamedi, W. H. Southwell, and W. J. Gunning, "Antireflection surfaces in silicon using binary optics technology," Appl. Opt. **31**, 4371-4375 (1992).

[9] T. K. Gaylord, W. E. Baird, and M. G. Moharam, "Zero-reflectivity high spatial frequency rectangular-groove dielectric surface-relief gratings," Appl. Opt. **25**, 4562-4567 (1986).

[10] Y. Ono, Y. Kimura, Y. Ohta, and N. Nishida, "Antireflection effect in ultrahigh spatial-frequency holographic relief gratings," Appl. Opt. **26**, 1142-1146 (1987).

[11] E. N. Glytsis and T. K. Gaylord, "Antireflection surface structure: dielectric layer(s) over a high spatial-frequency surface-relief gratings on a lossy substrate," Appl. Opt. **27**, 4288-4304 (1988).

[12] D. L. Brundrett, E. N. Glytsis, and T. K. Gaylord, "Homogeneous layer models for high- spatial-frequency dielectric surface-relief gratings: conical diffraction and antireflection designs," Appl. Opt. **33**, 2695-2706 (1994).

[13] D. H. Raguin and G. M. Morris, "Antireflection structured surfaces for the infrared spectral region," Appl. Opt. **32**, 1154-1167 (1993).

[14] D. H. Raguin and G. M. Morris, "Analysis of antireflection-structured surfaces with continuous one-dimensional surface profiles," Appl. Opt. **32**, 2582-2598 (1993).

[15] E. B. Grann, M. G. Moharam and D. A. Pommet, "Artificial uniaxial and biaxial dielectrics with use of two-dimensional subwavelength binary gratings," J. Opt. Soc. Am. **A11**, 2695-2703 (1994).

[16] E. B. Grann, M. G. Moharam and D. A. Pommet, "Optimal design for antireflective tapered two-dimensional subwavelength grating structures," J. Opt. Soc. Am. **A12**, 333-339 (1995).

[17] E. B. Grann and M. G. Moharam, "Comparison between continuous and discrete subwavelength grating structures for antireflection surfaces," J. Opt. Soc. Am. **A13**, 988-992 (1996).

[18] M. G. Moharam and T. K. Gaylord, "Diffraction analysis of dielectric surface-relief gratings," J. Opt. Soc. Am. **72**, 1385-1392 (1982).

[19] M. G. Moharam and T. K. Gaylord, "Three-dimensional vector coupled-wave analysis of planar-grating diffraction," J. Opt. Soc. Am. **73**, 1105-1112 (1983).

[20] M. G. Moharam, "Coupled-Wave Analysis of Two-dimensional Dielectric Gratings," Proc. Soc. Photo-Opt. Instrum. Eng. **883**, 8-11 (1988).

[21] S. T. Han, Y. Tsao, R. M. Walser, and M. F. Becker, "Electromagnetic scattering of two-dimensional surface-relief dielectric gratings," Appl. Opt. **31**, 2343-2352 (1992).

[22] D. Cho, "Eigenvalue problem pertaining to the rigorous three-dimensional vector coupled-wave analysis of diffraction from surface-relief gratings," Hankook Kwanghak Hoeji **5**, 439-444 (1994).

[23] netlib, Oak Ridge National Laboratory, Oak Ridge, TN, U. S. A.

[24] L. Li and C. W. Haggans, "Convergence of the coupled-wave methods for metallic lamellar diffraction gratings," J. Opt. Soc. Am. **A10**, 1184-1189 (1993).